



Life-Long Hyperbilirubinemia Exposure and Bilirubin Priming Prevent *In Vitro* Metabolic Damage

Annalisa Bianco^{1,2}, Serena Pinci^{1,2}, Claudio Tiribelli¹ and Cristina Bellarosa^{1*}

¹Italian Liver Foundation (FIF), Trieste, Italy, ²Department of Life Sciences, University of Trieste, Trieste, Italy

OPEN ACCESS

Edited by:

Terry D Hinds,
University of Kentucky, United States

Reviewed by:

David E. Stec,
University of Mississippi Medical
Center, United States
Andrew Bulmer,
Griffith University, Australia

*Correspondence:

Cristina Bellarosa
cristina.bellarosa@fegato.it

Specialty section:

This article was submitted to
Experimental Pharmacology and Drug
Discovery,
a section of the journal
Frontiers in Pharmacology

Received: 28 December 2020

Accepted: 15 February 2021

Published: 12 March 2021

Citation:

Bianco A, Pinci S, Tiribelli C and
Bellarosa C (2021) Life-Long
Hyperbilirubinemia Exposure and
Bilirubin Priming Prevent *In Vitro*
Metabolic Damage.
Front. Pharmacol. 12:646953.
doi: 10.3389/fphar.2021.646953

Background: Unconjugated bilirubin (UCB) is more than the final product of heme catabolism. Mildly elevated systemic bilirubin concentrations, such as in Gilbert syndrome (GS), protect against various oxidative stress-mediated and metabolic diseases, including cardiovascular disease, type 2 diabetes mellitus, metabolic syndrome, cancer, and age-related disease. The Gunn rat is an animal model of hereditary hyperbilirubinemia widely used in assessing the effect of high serum bilirubin concentration in various organs. The present work aims to understand if life-long hyperbilirubinemia and bilirubin-priming might contribute to protection against atherosclerosis and diabetic nephropathy (DN) at the cellular level.

Methods: Primary aortic endothelial cells and podocytes obtained from hyperbilirubinemic homozygous jj and normobilirubinemic heterozygous Nj Gunn rats were exposed to Palmitic Acid (PA) and Angiotensin II (Ang II), respectively, and the effects on cell viability and the activation of damage-related metabolic pathways evaluated. Results were validated on immortalized H5V and HK2 cells exposed to damage after UCB pretreatment.

Results: In both primary cell models, cells obtained from jj Gunn rats showed as significantly higher than Nj Gunn rats at any dose of the toxic agent. Reduction in CHOP expression and IL-6 release was observed in jj primary aortic endothelial cells exposed to PA compared to Nj cells. The same occurred on H5V pretreated with Unconjugated bilirubin. Upon Ang II treatment, primary podocytes from jj Gunn rats showed lower DNA fragmentation, cleaved caspase-3, and cleaved PARP induction than primary podocytes from Nj Gunn rats. In HK2 cells, the induction by Ang II of HIF-1 α and LOX12 was significantly reduced by UCB pretreatment.

Conclusion: Our data suggest that in models of atherosclerosis and DN life-long hyperbilirubinemia exposure or bilirubin-priming significantly contribute to decrease the injury by enhancing the cellular defensive response,

Keywords: Bilirubin, life-long hyperbilirubinemia, metabolic damage, apoptosis, inflammation, fibrosis, ER-stress

INTRODUCTION

Unconjugated bilirubin (UCB) is the final product of the heme catabolic pathway in the intravascular compartment. UCB is transported in the blood tightly bound to serum albumin before being taken up by the hepatocytes, where it is conjugated. The UCB fraction unbound to albumin (so-called free bilirubin, Bf) represents less than 0.1% and determines the biological properties of this pigment (Ahlfors et al., 2009). Bilirubin behavior in a human body has two faces, similar to the Janus Bifrons, a Roman god (Bianco et al., 2020). Elevated serum UCB concentration, and in particular the Bf fraction, exposes newborns to the risk of neurotoxicity (Watchko and Tiribelli, 2013). Conversely, mildly elevated systemic bilirubin concentrations, such as in Gilbert syndrome (GS) (Bosma et al., 1995), protect against various oxidative stress-mediated and metabolic disorders including cardiovascular disease, type 2 diabetes mellitus, metabolic syndrome, cancer, and age-related disease (Wagner et al., 2015; Vitek et al., 2018). These broad metabolic effects depend on the potent antioxidant activities, anti-inflammatory and immunomodulatory effects (Gazzin et al., 2016), and the recently described endocrine activity of UCB (Hinds Terry and Stec David, 2018; Hinds and Stec, 2019; Creeden et al., 2020; Vitek, 2020).

The partial deficiency of hepatic bilirubin UDP glucuronosyl transferase (UGT1A1) enzyme described in Gilbert patients, increases the unconjugated bilirubin level from 10 μ M (0.6mg/dl) to 20–70 μ M (1–5mg/dl) without any sign of liver damage (Vitek and Ostrow, 2009; Wagner et al., 2015). The Gunn rat is a model of hereditary hyperbilirubinemia widely used in assessing the effect of high serum bilirubin concentration in various organs. UCB concentration in hyperbilirubinemic homozygous jj Gunn rats (jj) serum (approximately from 2.42 to 7.36mg/dl) (Boon et al., 2012; Vianello et al., 2018) overlaps with elevated bilirubin concentrations seen in Gilbert subjects (Vitek et al., 2002; Bulmer et al., 2008; Boon et al., 2012). The UCB concentration in various organs and tissues of adult jj Gunn rats is higher than the normobilirubinemic heterozygous Nj Gunn rats (Nj) littermates. The UCB tissue content differs 131 fold in the myocardium (12.3ng/mg of tissue in jj vs. 0.093ng/mg of tissue in Nj) and 144 fold in the kidney (19.3ng/mg of tissue in jj vs. 0.134ng/mg of tissue in Nj) (Zelenka et al., 2008). The hyperbilirubinemia shown by jj Gunn rat is associated with marked anti-inflammatory (Wang et al., 2004), antiproliferative (Ollinger et al., 2005), antihypertensive (Pflueger et al., 2005), blood lipid-modulating properties (Wallner et al., 2013) and with fewer signs of cellular senescence (Zelenka et al., 2016). Moderate hyperbilirubinemia was demonstrated to lower (Ang II)-dependent hypertension by a mechanism that is partially dependent on the inhibition of superoxide production *in vivo* (Stec et al., 2013).

Atherosclerosis represents the major cause of cardiovascular diseases and it is caused by a combination of immune and inflammatory conditions leading to arterial wall injury (Zhang and Kaufman, 2008; Kang et al., 2014). The accumulation of cholesterol and free fatty acids (FFAs) in the ER membranes of macrophages causes calcium release, UPR activation, and

CHOP-induced apoptosis (Feng et al., 2003). Palmitic acid (PA) plays an important role in the development of atherosclerosis (Wu et al., 2014) due to its abundance as saturated fatty acid in FFAs (Lambertucci et al., 2008). The accumulation of PA in macrophages activates different transcriptional factors such as NF- κ B, thereby inducing the expression of genes encoding inflammatory cytokines including TNF- α and IL-6 (Zhang and Kaufman, 2008; Mazzone et al., 2009).

Diabetic nephropathy (DN) is a complication of diabetes mellitus and it is the leading cause of end-stage renal disease. The final effects of DN involve endothelial injury, tubulointerstitial fibrosis, and podocyte detachment and apoptosis (Maetzawa et al., 2015). Angiotensin II (Ang II) has been commonly used in *in vitro* modeling of DN as a pathophysiological mediator that mimics the disease (Slyne et al., 2015). HIF-1 α was recently identified as a promoter of kidney fibrosis (Haase, 2012) and has been demonstrated that its activation stimulates collagen accumulation and inflammatory cell recruitment in experimental model of CKD (Higgins et al., 2007; Kimura et al., 2008; Wang et al., 2011). While hypoxia is the main stimulus for HIF activation, Ang II have also been shown to activate HIF-1 α (Patten et al., 2010). LOX12 is considered an element of pro-fibrotic HIF-1 α pathway contributing to tubulointerstitial fibrosis development (Schietke et al., 2010). The early pathological changes of DN include podocyte apoptosis (Kume and Koya, 2015). Cleavage of PARP by caspase-3 is considered a hallmark of apoptosis (Jagtap and Szabó, 2005).

The present work aimed to understand if life-long hyperbilirubinemia and bilirubin-priming might have a protective effect in *in vitro models* of atherosclerosis and DN. The use of cellular models might help us to unravel the mechanisms associated with protection from renal injury and metabolic syndrome. Cells obtained from hyperbilirubinemic jj and normobilirubinemic Nj Gunn rats were exposed to damage in the absence of UCB. ER-stress and inflammation activation were evaluated on primary aortic endothelial cells exposed to PA to mimic atherosclerosis. Cell death by apoptosis was studied on primary podocytes exposed to Ang II to mimic diabetic nephropathy. Results were also validated on immortalized cell lines pretreated with UCB (bilirubin-priming) and then exposed to damage.

MATERIALS AND METHODS

Primary Cultures of Rat Podocytes and Aortic Endothelial Cells

Rats used in the project were born in the animal facility of the University of Trieste and animal handling was approved by the Ethics Committee for Animal Experimentation (OPBA) of the University of Trieste (NO1487BEL19) in compliance with the Italian regulation (D.L.vo 26/2014) and the Directive 2010/63/EU of the European Parliament. Hyperbilirubinemic jj and normobilirubinemic Nj Gunn rats were obtained by breeding a male homozygote (jj) with a female heterozygote (Nj). Rats were anesthetized by intraperitoneal injection of Zoletol (60mg/Kg)

and Xylazine (40mg/Kg) and successively sacrificed through decapitation. 90% of rats used were male, but we did not distinguish between males and females. Rats were sacrificed when reached a weight around 200gr, corresponding to 8weeks for males and 10weeks for females..

The kidneys were extracted and conserved in D-glucose (5.5mM) Dulbecco's Modified Eagle's Medium (DMEM) and Ham's F12 medium (Euroclone S. p.A., Milano, Italy) in the ratio 1:1 on ice; Bowman's capsule was removed by pliers (Rush et al., 2018) and the cortical region of the organ was cut into thin strips. Glomeruli were collected in 50ml DMEM/F12 solution using filters with different sizes (80, 100, and 300 meshes) (Sigma-Aldrich, St. Louis MO, United States) and a pestle. They were then centrifuged at 136g for 5min at room temperature. The pellet was seeded in the 25cm² culture flasks pre-coated with collagen type IV (Sigma-Aldrich, St. Louis MO, United States). Glomeruli were left in the incubator at 37°C in 5% CO₂ humidified atmosphere in a medium composed by DMEM low glucose and Ham's F12 media (1:1) supplemented with a final concentration of deplemented 10% (v/v) FBS, 1% penicillin/streptomycin solution (penicillin G (100U/mL), streptomycin (100mg/ml)), L-glutamine (2mmol/L), bovine insulin (5mg/ml), 5µg/ml holo-transferrin (5mg/ml), sodium selenite (5ng/ml) and hydrocortisone (5ng/ml) (Sigma-Aldrich, St. Louis MO, United States) (Zennaro et al., 2014). After 4/5days of incubation podocytes began to emerge and grow out from the glomeruli and, once reached 70–80% of confluence, they were detached using trypsin-EDTA (Euroclone S.p.A., Milano, Italy) and scraper, and collected using a 40-mesh filter. Finally, they were seeded in the 25cm² culture flasks pre-coated with collagen type IV (Sigma-Aldrich, St. Louis MO, United States).

The aorta was extracted and conserved in Human Endothelial serum-free medium GIBCO (Life Technologies, Monza, Italy). The aorta (approximately 2cm long) was cleaned from fat tissue, cut into two halves longitudinally, and digested by collagenase type II (2mg/ml) (Worthington Industries, OH, United States). After collagenase treatment, endothelial cells removed from the aorta were collected by centrifugation and suspended in 10ml of Human Endothelial medium GIBCO (Life Technologies, Monza, Italy) supplemented with a final concentration of 10% FBS, EGF (10ng/ml), bFGF 20ng/ml, and 1% penicillin/streptomycin solution (penicillin G (100U/mL) in 5 wells (2ml/well) of 6-multiwell coated with gelatin. After 1h of incubation at 37°C, the supernatant containing endothelial cells was re-seeded in another well. Then aortic endothelial cells were isolated and characterized by magnetic beads coated with CD31 (BD Biosciences, San Jose, CA), a characteristic marker for endothelial cells (Liu et al., 2008).

Immortalized Cell Culture

HK2, an immortalized human proximal tubular epithelial cell line (kindly provided by Prof. R. Bulla, Department of Life Sciences, University of Trieste), was cultured in DMEM low glucose and Ham's F12 media (1:1) supplemented with a final concentration of deplemented 5% (v/v) FBS, 1% penicillin/streptomycin solution (penicillin G (100U/mL), streptomycin (100mg/ml)), L-glutamine (2mmol/L), bovine insulin (5mg/ml), holo-transferrin (5mg/ml), sodium selenite

(5ng/ml), hydrocortisone (5ng/ml), EGF (10ng/ml), T3 (5pg/ml), and PGE (15pg/ml).

H5V, murine heart endothelial cells transformed by polyomavirus middle T-antigen (kindly provided by Istituto Mario Negri, Milan, Italy) were grown in DMEM low glucose containing a final concentration of 10% (v/v) FBS, 1% penicillin/streptomycin solution (penicillin G (100U/mL), streptomycin (100mg/ml)), and L-glutamine (2mmol/L).

Once reached 80% of confluence, both the cell lines were employed for the experimental studies as described below.

Treatments

UCB Treatment

UCB (Sigma-Aldrich, St. Louis MO, United States) was purified as previously described (McDonagh and Assisi, 1972) and dissolved in DMSO to reach a final concentration of 6mM. To reach the final concentrations desired, UCB was serially diluted with DMSO and then with a growth medium. All UCB treatments were performed in the presence of BSA 30µM. The solvent was always 0.1% (v/v) in all bilirubin concentrations used. DMSO 0.1% was used to treat control cells. H5V and HK2 UCB pretreatment were performed in cell culture medium in the presence of BSA 30µM with total UCB concentrations of 1.25 and 2.5µM. According to Roca et al. (2006), these concentration correspond to a Bf < 15nM and = 15nM, respectively. These concentrations of Bf were chosen since they are similar to the plasma Bf levels found in humans with mild unconjugated hyperbilirubinemia (Jacobsen and Wennberg, 1974; Nelson et al., 1974).

Angiotensin II Treatment

Human Angiotensin II (Sigma-Aldrich, St. Louis MO, United States) was reconstituted with phosphate-buffered saline (PBS) at the concentration of 1mg/ml. The range of angiotensin II concentration used in the experiments ranged from 0.01µM up to 10µM and all treatments required 24h (Chen et al., 2017).

Palmitic Acid Preparation and Treatment

Palmitic acid (PA) 0.1M stock solutions were prepared by dissolving fatty acid-free (FFAs) in DMSO. The cells were exposed for 24h. Since albumin played a crucial role in determining the FFAs available concentration, the BSA concentration was kept fixed at 75µM. The FFAs were complexed with bovine serum albumin at a different molar ratio. The medium containing BSA 75µM was aliquoted to set up various BSA/PA ratios (1:1, 1:2, 1:3, 1:4, 1:5, 1:6). DMSO solution was used as control and its final concentration never exceeded 0.1%.

Cytotoxicity Test (PI) and Metabolic Activity Test (MTT)

Both the cytotoxicity test and metabolic activity test were performed in black 96-well plates. Propidium iodide (PI) (Sigma-Aldrich, St. Louis MO, United States) was solubilized in PBS to a final concentration of 50µg/ml. After 60min of

incubation at 37°C, the initial fluorescence intensity due to the dead cells was measured using a multiplate reader (EnSpire 2300, PerkinElmer, MA, United States). The excitation and the emission wavelengths were 530 and 620nm, respectively. After the measurement, Triton X-100 at a final concentration of 0.6% was added to each well to permeabilize the cells and let PI label cell nuclei. After 30min of incubation on ice, fluorescence intensity was re-measured to obtain a value corresponding to the total cells. The percentage of dead cells was calculated as the proportion of fluorescence intensity of dead cells to that of total cells.

Metabolic activity was determined by assessing the reduction of 3 (4,5-dimethyl thiazolyl-2)-2,5 diphenyl tetrazolium (MTT, Sigma-Aldrich, St. Louis MO, United States) to formazan by succinate dehydrogenase, a mitochondrial enzyme. In brief, a stock solution of MTT was prepared in PBS (5mg/ml) and then diluted to 0.5mg/ml in the cell medium. Cells were incubated with the cell medium containing MTT for 1h at 37°C. At the end of the incubation time, the insoluble formazan crystals were dissolved in 100µL of DMSO. Absorbance was determined at 562nm by using a multiplate reader (EnSpire 2300, PerkinElmer). The results were expressed as the percentage of control cells not exposed to UCB, which were considered as being 100% viable. It is important to note that MTT test is a quantitative colorimetric assay to detect the survival and proliferation rate of living cells (Mosmann, 1983).

Total Protein Extractions, Quantification, and Western Blot Analysis

Cells were treated when they reached a confluence of approximately 80%. Total proteins were extracted by lysing the cells in an ice-cold cell lysis buffer (Cell Signaling Technology, MA, United States). The protein concentration was determined by the bicinchoninic acid protein assay (BCA) according to manufacturer's instructions. Equal amounts of protein were separated by SDS-polyacrylamide gel electrophoresis (SDS-PAGE) and transferred to PVDF membranes (Bio-Rad Laboratories, CA, United States). Membranes were blocked in 4% milk or 4% BSA in T-TBS (0.2% Tween 20, 20 mM Tris-HCl (pH 7.5) and 500 mM NaCl) and incubated overnight at 4°C with the primary antibodies: Anti-HIF-1α antibody (GeneTex, CA, United States), Anti-LOX2 antibody (CUSABIO Technology LLC, TX, United States), Anti-PARP antibody (Cell Signaling Technology, MA, United States), Anti-CHOP antibody (Invitrogen, Carlsbad, United States) Anti-Caspase-3 antibody (Pro and Cleaved forms) (Thermo Fisher Scientific, MA, United States) and anti-Actin (Sigma-Aldrich, St. Louis MO, United States). Membranes were then incubated with anti-rabbit or anti-mouse secondary antibodies (Dako Laboratories, CA, United States). Protein bands were detected by peroxide reaction using ECL Plus Western Blot detection system solutions (ECL Plus Western Blot detection reagents, GE-Healthcare Bio-Sciences). The relative intensity of protein bands was scanned and analyzed using the C-DiGit® Blot Scanner—LI-COR (Biosciences). The optical density of the bands of interest was normalized to α-Actin and represented as relative to DMSO-treated cells.

Immunofluorescence

Podocytes were seeded onto appropriate glass coverslips pre-coated with poly-L-lysine (Sigma Aldrich, United States) and fixed with 4% paraformaldehyde. A permeabilization step was performed using 0.5% Triton X-100 for 5min. After being blocked with 5% bovine serum albumin (BSA) in PBS-T + 0.1% Tween 20 for 60min at room temperature, the coverslips were incubated with the primary antibody rabbit anti-nephrin (Sigma-Aldrich, St. Louis MO, United States) or anti-Cleaved Caspase-3 antibody (Elabscience, TX, United States) overnight at 4°C. The coverslips were washed thoroughly in PBS and incubated with Alexa Fluor 546 goat anti-rabbit (Invitrogen, Carlsbad, CA, United States) in the dark for 1h at room temperature. After appropriate washes, cell nuclei were stained with Hoechst 33,328 (Sigma-Aldrich, St. Louis MO, United States) at room temperature. Cells were mounted with Fluorescent Mounting Media (Calbiochem, San Diego, CA, United States) and images were acquired using a Leica DM 2000 microscope equipped with an appropriate filter to cover both the excitation and emission wavelengths of Alexa Fluor 546 and Hoechst 33,328. In each experimental setting, images were captured with identical light exposure parameters and aperture settings.

TUNEL Assay

For *in situ* detection of DNA fragmentation, the Click-iT™ Plus TUNEL Assay was used following the manufacturer's protocol (Thermo Fisher Scientific, MA, United States).

IL-6 ELISA

The supernatants of H5V and Aortic endothelial primary cells were collected and subjected to ELISA analysis using Mouse IL-6 ELISA KIT (Diacione, Besançon, Francia) and Rat IL-6 ELISA KIT (Thermo Fisher Scientific, MA, United States) respectively, following the manufacturer's instructions.

Statistical Analysis

GraphPad Prism 5 software (GraphPad, San Diego, CA, United States) was used to perform statistical analysis. A statistically significant difference between two data sets was assessed by unpaired two-tailed Student's t-test. Data were obtained from at least three independent experiments and were expressed as mean ± SD. Significance was graphically indicated as follows: * $p < 0.05$, ** $p < 0.01$, *** $p < 0.001$.

RESULTS

PA and Angiotensin II Impact on Cell Viability in Nj and jj Primary Cells

Aortic endothelial cells harvested from Nj and jj Gunn rats were treated for 24h with increasing doses of PA ranging from 75µM up to 450µM in the presence of 75µM BSA. As shown in **Figure 1A**, upon 75µM PA Nj cells showed a 30% reduction of their viability of as compared to 15–20% jj cells'. A significantly higher (* $p < 0.05$, *** $p < 0.001$) viability of jj-derived was found at any PA concentration.

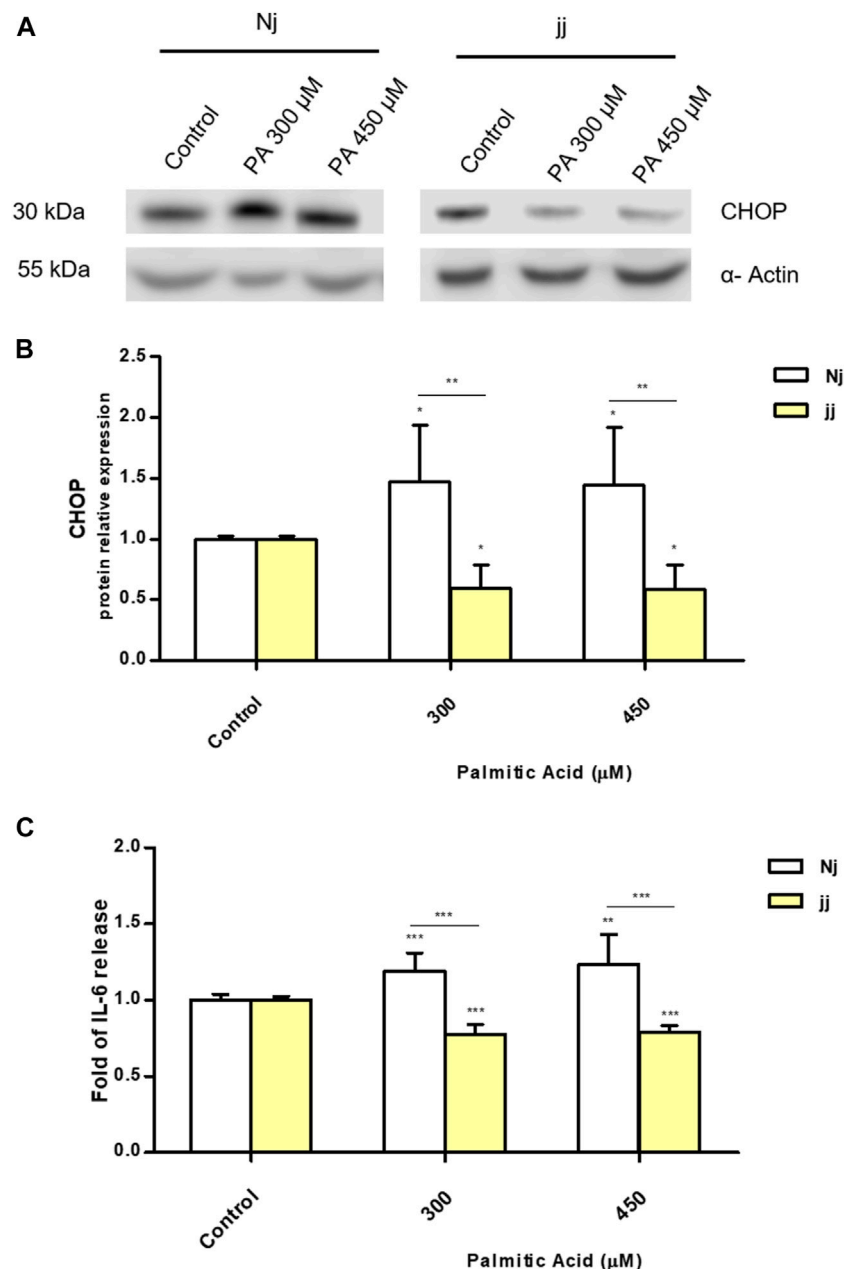
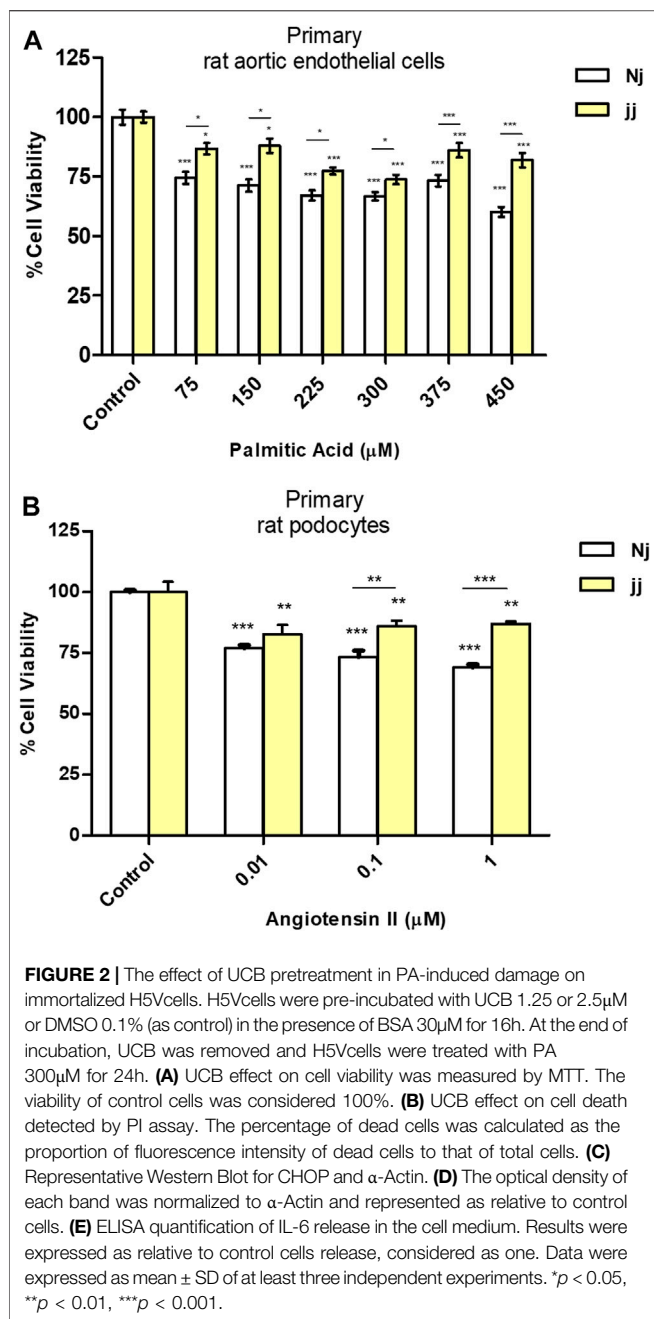


FIGURE 1 | Effect of PA and Ang II treatments on cell viability (MTT test) in normobilirubinemic (Nj) and hyperbilirubinemic (jj) primary cells. **(A)** Aortic endothelial primary cells were exposed to increasing PA concentrations (from 75 to 450 μ M in the presence of 75 μ M BSA) for 24h. Cells treated with complete growth medium were considered 100% of viability. Data were expressed as mean \pm SD of six independent experiments. **(B)** Primary podocytes were exposed to the Ang II 0.01, 0.1, and 1 μ M for 24h. Cells treated with complete growth medium were considered 100% of viability. Data were expressed as mean \pm SD of three independent experiments. * p < 0.05, ** p < 0.01, *** p < 0.001.

Primary podocyte characterization by immunofluorescence indicated a highly elevated level of nephrin protein with a plasma membrane and perinuclear co-localization (**Supplementary Figure S1**). The viability of primary podocytes exposed to Ang II 0.01, 0.1, and 1 μ M for 24h (**Figure 1B**) was significantly (** p < 0.01, *** p < 0.001) reduced at any Ang II concentration (20–25% vs. 10–15% in Nj and jj podocytes.)

The effect of bilirubin priming on cell viability was also evaluated on immortalized cell lines. Heart endothelial cells (H5V) were first exposed to 1.25 or 2.5 μ M UCB for 16h and then exposed to increasing doses of PA for 24h. As shown in **Figure 2** panel A and B, while PA treatment reduced cell viability by approximately 50% and increased cell death up to 20%, UCB pretreatment increased cell viability and reduced the cell death rate. Immortalized human proximal tubular epithelial cells (HK-



2) were exposed to increasing Ang II concentration (0.01–10μM for 24h). Even if Ang II treatment affected podocytes cell viability, as expected (Baker and Kumar, 2006), there was no change on HK2 cell viability or cell mortality compared to control, when exposed to Ang II (Supplementary Figures S2A and S2B).

PA Impact on CHOP Activation and IL-6 Release in Nj and jj Aortic Endothelial Primary Cells

We investigated the metabolic pathways involved in aortic endothelial cell viability focusing on ER stress and

inflammation. Primary endothelial Nj and jj cells were treated with PA 300 and 450μM for 24h. A significant up-regulation of CHOP protein was observed after 24h of incubation with PA 300 and 450μM only in Nj aortic endothelial cells (*p* < 0.05). Conversely, the same treatment on jj showed a significant decrease in CHOP protein level (*p* < 0.05) (Figures 3A,B). A boost in IL-6 production upon PA 300μM and PA 450μM treatments was observed only in Nj cells, while cells from jj rats showed a significant decrease in IL-6 release (*p* < 0.001). The IL-6 release in the cell medium by jj cells was significantly lower than that released by cells from Nj rats (*p* < 0.001) (Figure 3C).

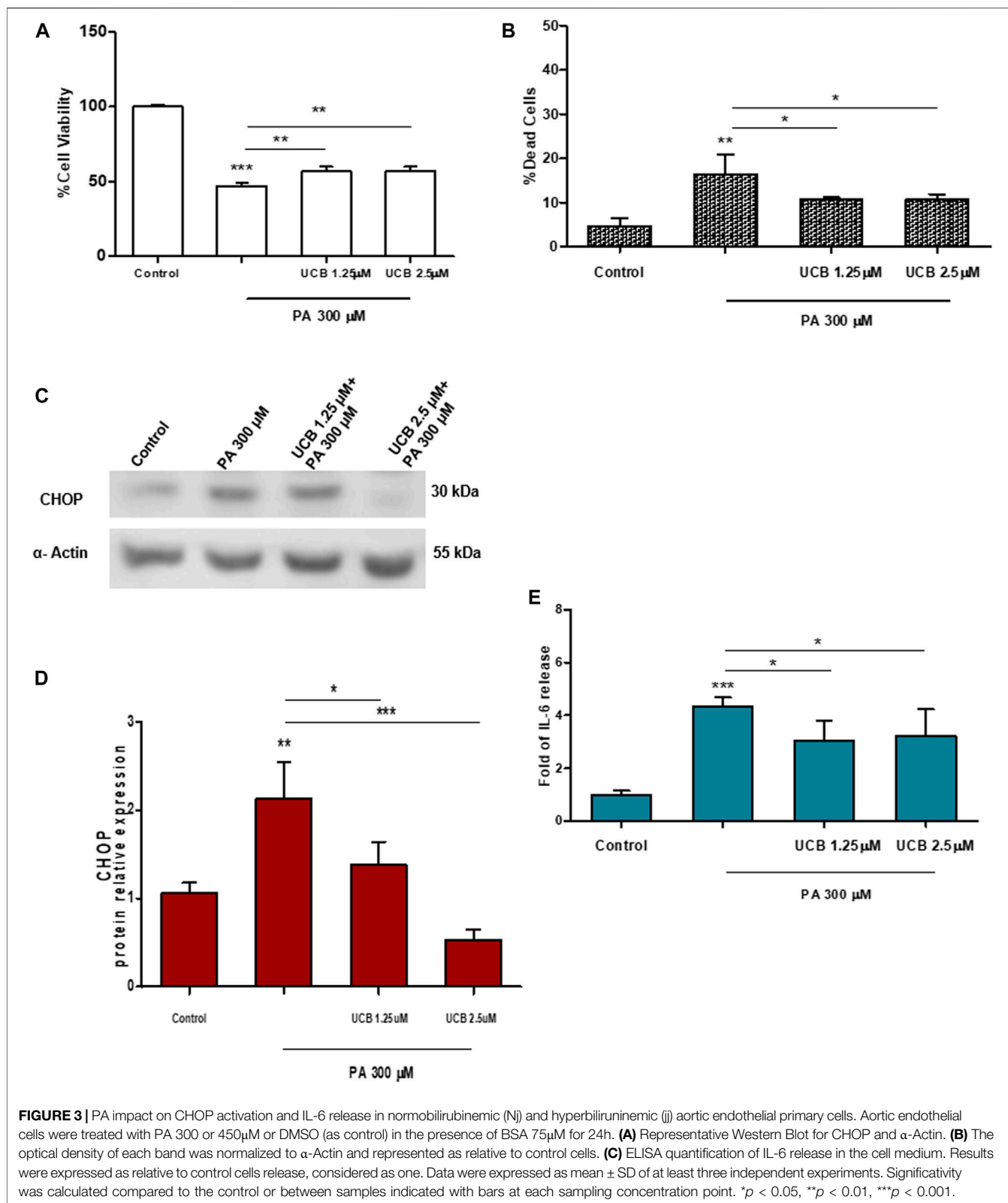
Similar results were observed in H5Vcells. Cells were first treated with UCB1.25 or 2.5μM for 16h and then exposed to PA 300μM for 24h. 300μM PA treatment significantly increased the expression level of CHOP protein (*p* < 0.01) while UCB pretreatment restores it to the control level (Figures 2C,D). Similarly, UCB pretreatment significantly (*p* < 0.05) reduced PA 300μM increase of IL-6 release (Figure 2E).

Angiotensin II Impact on Apoptosis Activation in Nj and jj Podocyte Primary Cells

Treatment with Ang II 0.01, 0.1, and 1μM for 24h showed a significant increase in the number of apoptotic podocytes in both genotypes, as detected by TUNEL assay (Figure 4A). However, the extent of Ang II-induced apoptosis was greater in podocytes harvested from Nj rats compared to the podocytes of jj rats at each Ang II concentration tested (Figure 4B). In normobilirubinemic podocytes, Ang II treatment induced a dose-dependent increase in cleaved caspase-3 expression assessed by immunofluorescence. Conversely, only 1μM Ang II significantly increased the expression of cleaved caspase-3 in jj podocytes (*p* < 0.001). Caspase-3 activation significantly (*p* < 0.01) differed between the two genotypes upon all Ang II treatments (Figures 5A,B). Due to the limited yield of total protein obtained from primary podocyte cultures, WB analysis was performed only on Ang II 0.01 and 0.1μM treatments for cleaved PARP and cleaved caspase-3 (Figure 5C). Both treatments induced an almost two-fold increase in the protein level of activated caspase-3 only in cells from Nj rats, while the expression remained similar to control levels in podocytes from jj rats (Figure 5D). The cleaved PARP expression was slightly induced in podocytes from Nj rats, while its expression is reduced compared to control cells in podocytes from jj rats (Figure 5E).

Impact of UCB on Fibrosis Induced by Angiotensin II in Proximal Tubular Epithelial Cells

Ang II is known to induce fibrosis in tubular epithelial cells. A dose-dependent increase of HIF-1α and LOX12 protein expression was detected on immortalized human proximal tubular epithelial cells (HK-2) exposed to increasing concentration of Ang II for 24h. Treatment with Ang II concentrations 0.5 and 1μM showed a significant (*p* < 0.05)



up-regulation of HIF-1 α protein expression while LOX12 protein expression was significantly ($p < 0.05$) up-regulated by AngII 0.05 μ M (Figures 6A,B). Moreover, the effects of Ang II on HIF-

1 α mRNA expression did not show any variation compared to controls (data not shown). Considering the induction of HIF-1 α and LOX12 protein by Ang II, we investigated whether UCB

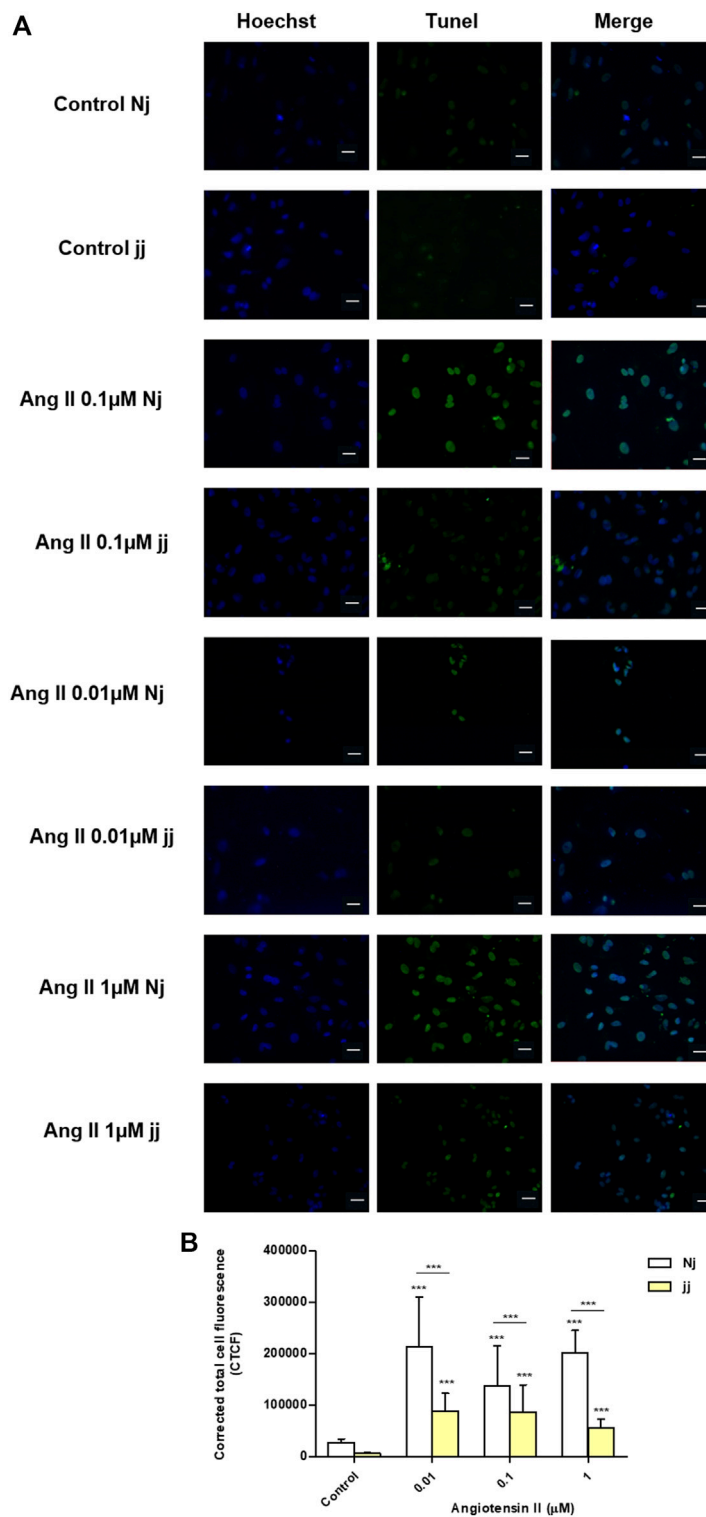


FIGURE 4 | TUNEL staining of normobilirubinemic (Nj) and hyperbilirubinemic (jj) Gunn rat primary podocytes exposed to Ang II treatments. Primary podocytes were exposed to Ang II 0.01, 0.1, and 1 μM for 24h. Cells treated with complete growth medium were considered as control. **(A)** Apoptotic cells were detected by TUNEL assay. Green fluorescence indicated TUNEL-positive and blue indicated Hoechst nuclear dye. Magnification ×40. Scale bar 50 μm. **(B)** Quantification of fluorescence intensity. The fluorescence intensity was quantified using ImageJ and displayed as corrected total cell fluorescence (CTCF). Results shown represented the mean ± SD of three independent experiments. Significativity was calculated compared to the control or between samples indicated with bars at each sampling concentration point. **p* < 0.05, ***p* < 0.01, ****p* < 0.001.

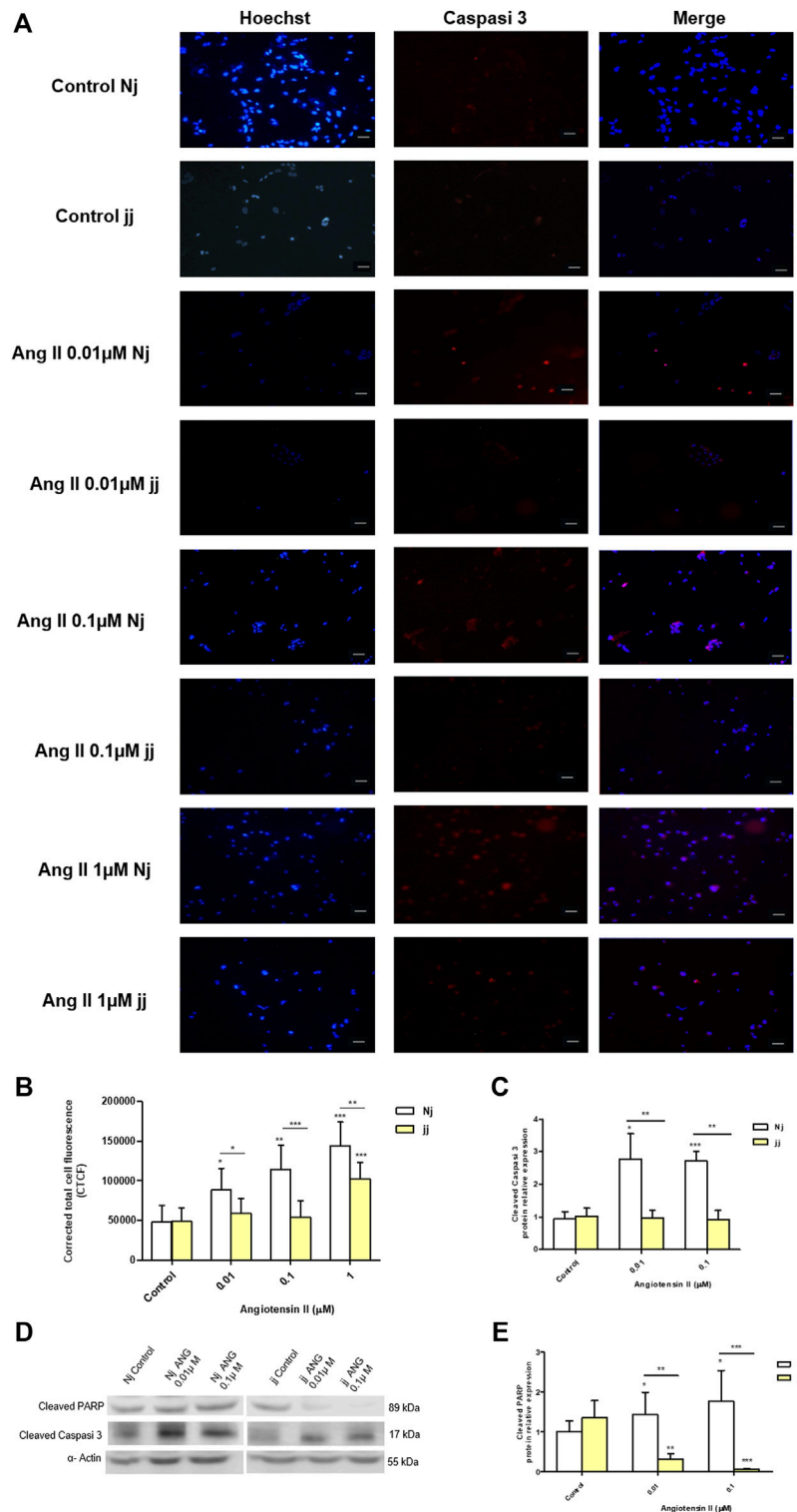
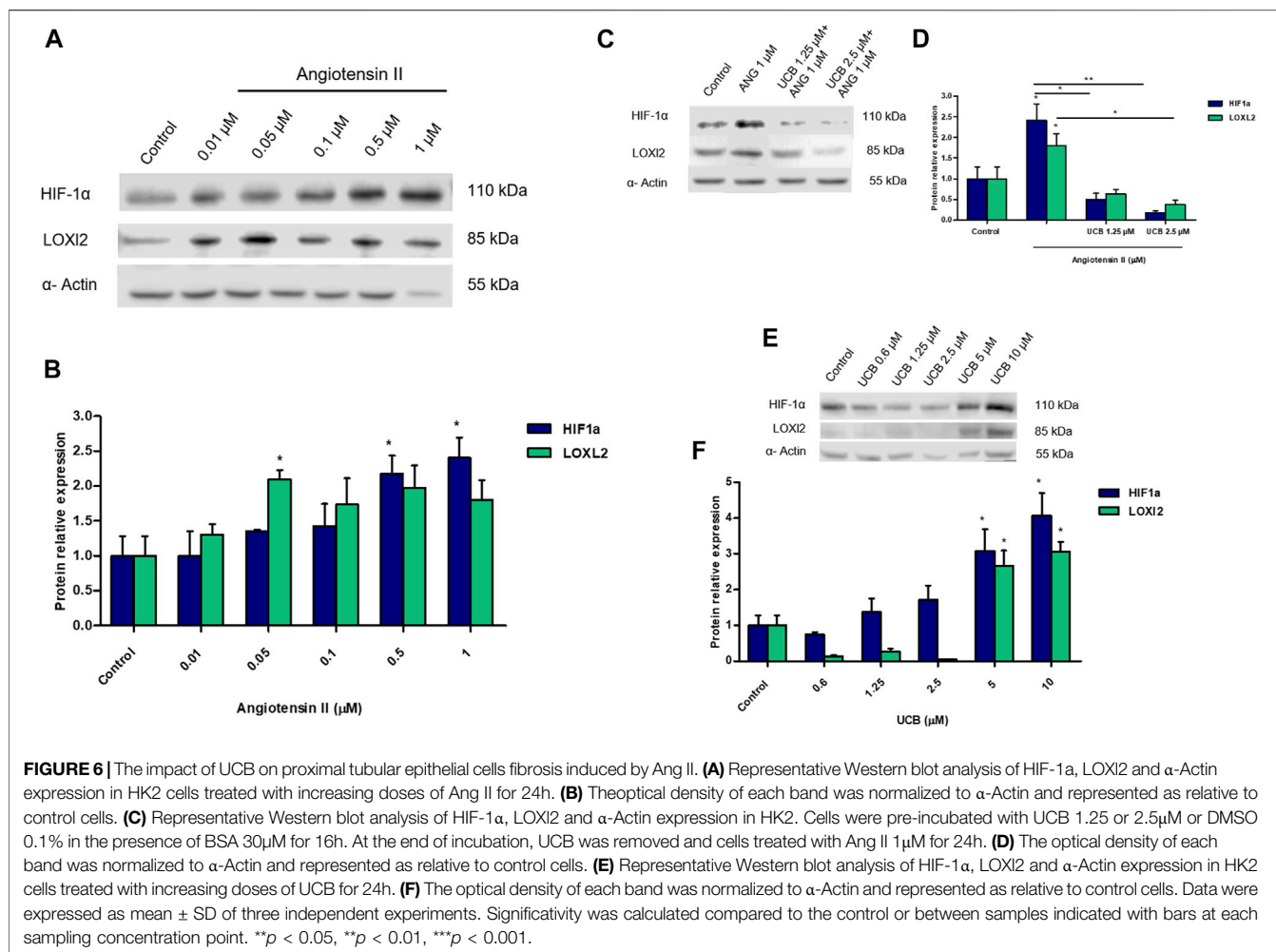


FIGURE 5 | Activation of apoptosis signaling by Ang II in normobilirubinemic (Nj) and hyperbilirubinemic (jj) podocytes primary cells. Primary podocytes were exposed to Ang II 0.01, 0.1, and 1µM for 24h. Cells treated with complete growth medium were considered as control. **(A)** Representative immunofluorescence ($n = 3$) images showing immunostaining for cleaved Caspase-3 (red) and Hoechst (blue) for nuclei. Magnification $\times 20$. Scale bar 50µm. **(B)** Quantification of Cleaved Caspase-3 fluorescence intensity. The fluorescence intensity was quantified using ImageJ and displayed in corrected total cell fluorescence (CTCF). **(C)** Representative Western blot analysis of cleaved PARP, cleaved caspase-3 and α -Actin expression in total cell lysates. **(D)** The optical density of cleaved caspase-3 protein from three independent experiments was normalized to α -Actin and represented as relative to untreated cells. **(E)** The optical density of cleaved PARP protein from three independent experiments was normalized to α -Actin and represented as relative to untreated cells. Significativity was calculated compared to the control or between samples indicated with bars at each sampling concentration point. * $p < 0.05$, ** $p < 0.01$, *** $p < 0.001$.



pretreatment may influence its expression. Pretreatment with 1.25 μ M or 2.5 UCB significantly reduced HIF-1 α protein induction by AngII in a dose-dependent manner ($p < 0.05$, $p < 0.01$). UCB also significantly ($p < 0.05$) reduced LOX12 protein to 0.5-fold of control cells (Figures 6C,D). The effect of UCB alone on HIF-1 α and LOX12 protein expression was evaluated by exposing for 24h HK2 cells to a dose-dependent UCB treatment (from 0.6 to 10 μ M). HIF-1 α and LOX12 expression was reduced by UCB treatment up to 2.5 μ M, while higher concentration induced their expression (Figures 6E,F).

DISCUSSION

Several studies showed the protective effect of bilirubin against oxidative-stress based disease. In the present work, we assessed if life-long hyperbilirubinemia and bilirubin-priming might significantly contribute to the protection against metabolic insult *in vitro*. To this goal, we used primary cells obtained from hyperbilirubinemic jj and normobilirubinemic Nj Gunn rats exposed to damaging agents. Primary cells from jj Gunn rats were more viable and less prone to damage compared to cells

from Nj Gunn rats, suggesting a modulating activity on cellular signaling of a life-long hyperbilirubinemia. This conclusion was further supported by data obtained in immortalized cell lines pretreated with UCB (bilirubin-priming) and then exposed to damage.

Studies comparing the response to damage between primed and not primed UCB cells are scant. Recently Valaskova et al. showed that the cell viability of primary hepatocytes from jj Gunn rats exposed to TNF- α 100ng/ml was significantly higher than that of primary hepatocytes from Nj Gunn rats ($p < 0.05$) (Valaskova et al., 2019). Our results expand this observation as we assayed the viability of other primary cell types (podocytes and primary aortic endothelial cells) exposed to increasing concentration of a damaging stimulus (PA and Ang II, respectively). In both cell models and at any toxic agent concentration, the viability of cells derived from jj Gunn rats was significantly higher than that of Nj cells. In line with this, UCB pretreatment in H5V cells exposed to PA reduced the percentage of dead cells and increased cell viability compared to DMSO pretreated cells. Bilirubin activates various nuclear and cytoplasmic receptors, resembling the endocrine activities of hormonal substances. This is true both for the "classic" hepatic nuclear receptors, and for some lesser-explored receptors or other

signaling molecules (Vítek, 2020). We previously showed that 24h of bilirubin-priming modulates the glutathione levels in neuroblastoma cells through the induction of the System Xc-, and this renders the cell less prone to oxidative damage (Giraudi et al., 2011).

Bilirubin exerts potent anti-inflammatory and immunomodulatory activities (Jangi et al., 2013) and the interrelation between UCB, ER-Stress, inflammation, and associated cascade of events has been demonstrated (Barateiro et al., 2012). An increasing body of evidence suggests that mildly elevated bilirubin level could control inflammation, both *in vitro* and *in vivo*, through the mechanisms involved in NF- κ B signaling pathway inhibition as well as the activation of inflammasomes (Li et al., 2020) suppressing the production of pro-inflammatory cytokines (Liu et al., 2008; Adin et al., 2017). We observed a reduced CHOP expression and IL-6 release in jj aortic endothelial primary cells exposed to PA compared to cells from Nj rats. Besides, in immortalized H5V cell line pretreatment with UCB significantly reduced CHOP expression and IL-6 release induced by PA treatment. Of notice, the TNF- α -stimulated nuclear translocation of NF- κ B was inhibited by UCB in H5V cells (Mazzone et al., 2009). Co-treatment with UCB resulted in reducing ER-stress and the subsequent inflammatory response also in *in vitro* model of gut inflammation (Gundamaraju et al., 2019). The anti-inflammatory and anti-oxidative effects may likely contribute to the protective role of bilirubin on vascular damage (Inoguchi et al., 2016).

Diabetic nephropathy (DN) is a complication of diabetes mellitus and is the leading cause of end-stage renal disease. The final effects of diabetic nephropathy involve endothelial injury, tubule-interstitial fibrosis, and podocytes detachment and apoptosis (Maezawa et al., 2015). Bilirubin provided a nephroprotective effect in different *in vivo* models as showed by the finding that jj Gunn rats showed significantly lower creatinine compared with Wistar rats at day 5 in a cisplatin nephrotoxicity model (Barabas et al., 2008). In streptozotocin-induced diabetic damage, jj Gunn rats exhibited significantly less urinary albumin excretion, did not develop renal mesangial expansion, and expressed lower levels of TGF- β and fibronectin than diabetic Nj Gunn rats (Fujii et al., 2010). We found that, upon Ang II treatment, primary podocytes from jj Gunn rats showed lower DNA fragmentation, cleaved caspase-3, and cleaved PARP induction than primary podocytes from Nj Gunn rats. Also, on the cyclosporine (CsA)-induced nephropathy rat model, a significantly lower number of apoptotic cells was observed in the bilirubin-treated rat kidneys compared to controls, confirming the bilirubin anti-apoptotic effect (Oh et al., 2013).

Recent studies have proposed for HIF-1 α downstream function of a pro-fibrotic signaling cascade stimulated by angiotensin II, leading to epithelial-mesenchymal transition and excessive collagen apposition (Wang et al., 2011). We found that Ang II acts as a pro-fibrotic marker inducing HIF-1 α and LOX12 protein expression in a dose-dependent manner. Expanding the previous evidence (Kim et al., 2014), we showed that bilirubin modulated the expression of the pro-fibrotic marker with double-side behavior. UCB treatment up to 2.5 μ M decreased HIF-1 α and LOX12 expression compared to control, while higher UCB concentration induced their expression. This is due to the extent of intracellular UCB concentration which determines the UCB anti- or pro-oxidant effect (Bianco et al., 2020). HIF-1 α and

LOX12 protein induction by Ang II was significantly reduced by UCB pretreatment of 1.25 or 2.5 μ M corresponding to an antioxidant intracellular UCB concentration (Bianco et al., 2020). Bilirubin has been shown to have an anti-fibrotic effect on cyclosporine (CsA)-induced nephropathy *in vivo*, given that bilirubin pretreatment significantly improved afferent arteriopathy, tubulointerstitial fibrosis, and tubular injury compared to the CsA-only treated rats (Oh et al., 2013).

Our data suggest that life-long hyperbilirubinemia exposure and bilirubin-priming significantly contribute to increase cell viability and enhance responses to damage in *in vitro* models of atherosclerosis and DN. Collectively these findings further support the beneficial effect of bilirubin on different organs.

DATA AVAILABILITY STATEMENT

The original contributions presented in the study are included in the article/**Supplementary Material**, further inquiries can be directed to the corresponding author.

ETHICS STATEMENT

The animal study was reviewed and approved by the Ethics Committee for Animal Experimentation (OPBA), University of Trieste.

AUTHOR CONTRIBUTIONS

AB and CB designed the study. AB, SP, and CB performed experiments and data analysis. AB, SP, CT, and CB interpreted the findings, prepared, and completed the manuscript. CT revised the final version. All authors contributed to the article and approved the submitted version.

FUNDING

This work has been supported in part by Beneficentia Stiftung, Banca d'Italia, and FIF internal grants.

ACKNOWLEDGMENTS

The authors want to thank Deborah Bonazza e Cristina Bottin for IHC of rat aorta and kidney; Cristina Zennaro for teaching how to prepare primary rat podocytes; Fluer Bossi for helping in the setup or rat aortic endothelial isolation.

SUPPLEMENTARY MATERIAL

The Supplementary Material for this article can be found online at: <https://www.frontiersin.org/articles/10.3389/fphar.2021.646953/full#supplementary-material>.

REFERENCES

- Adin, C. A., VanGundy, Z. C., Papenfuss, T. L., Xu, F., Ghanem, M., Lakey, J., et al. (2017). Physiologic doses of bilirubin contribute to tolerance of islet transplants by suppressing the innate immune response. *Cell Transpl.* 26, 11–21. doi:10.3727/096368916X692096
- Ahlfors, C. E., Wennberg, R. P., Ostrow, J. D., and Tiribelli, C. (2009). Unbound (free) bilirubin: improving the paradigm for evaluating neonatal jaundice. *Clin. Chem.* 55, 1288–1299. doi:10.1373/clinchem.2008.121269
- Baker, K. M., and Kumar, R. (2006). Intracellular angiotensin II induces cell proliferation independent of AT1 receptor. *Am. J. Physiol. Cell Physiol.* 291, C995–C1001. doi:10.1152/ajpcell.00238.2006
- Barabas, K., Milner, R., Farese, J., Baylis, C., Croker, B., Archer, L., et al. (2008). Hyperbilirubinemia's protective effect against cisplatin nephrotoxicity in the Gunn rat. *Anticancer Drugs* 19, 495–502. doi:10.1097/CAD.0b013e3282fcd391
- Barateiro, A., Vaz, A. R., Silva, S. L., Fernandes, A., and Brites, D. (2012). ER stress, mitochondrial dysfunction and calpain/JNK activation are involved in oligodendrocyte precursor cell death by unconjugated bilirubin. *Neuromolecul. Med.* 14, 285–302. doi:10.1007/s12017-012-8187-9
- Bianco, A., Dvořák, A., Capková, N., Gironde, C., Tiribelli, C., Furger, C., et al. (2020). The extent of intracellular accumulation of bilirubin determines its anti-oxidant effect. *Int. J. Mol. Sci.* 21. doi:10.3390/ijms21218101
- Boon, A.-C., Hawkins, C. L., Bisht, K., Coombes, J. S., Bakrania, B., Wagner, K.-H., et al. (2012). Reduced circulating oxidized LDL is associated with hypocholesterolemia and enhanced thiol status in Gilbert syndrome. *Free Radic. Biol. Med.* 52, 2120–2127. doi:10.1016/j.freeradbiomed.2012.03.002
- Bosma, P. J., Chowdhury, J. R., Bakker, C., Gantla, S., de Boer, A., Oostra, B. A., et al. (1995). The genetic basis of the reduced expression of bilirubin UDP-glucuronosyltransferase 1 in Gilbert's syndrome. *N. Engl. J. Med.* 333, 1171–1175. doi:10.1056/NEJM199511023331802
- Bulmer, A. C., Blanchfield, J. T., Toth, I., Fassett, R. G., and Coombes, J. S. (2008). Improved resistance to serum oxidation in Gilbert's syndrome: a mechanism for cardiovascular protection. *Atherosclerosis* 199, 390–396. doi:10.1016/j.atherosclerosis.2007.11.022
- Chen, L., Chen, D.-Q., Wang, M., Liu, D., Chen, H., Dou, F., et al. (2017). Role of RAS/Wnt/ β -catenin axis activation in the pathogenesis of podocyte injury and tubulo-interstitial nephropathy. *Chem. Biol. Interact.* 273, 56–72. doi:10.1016/j.cbi.2017.05.025
- Creeden, J. F., Gordon, D. M., Stec, D. E., and Hinds, T. D. (2020). Bilirubin as a metabolic hormone: the physiological relevance of low levels. *Am. J. Physiol. Endocrinol. Metab.* doi:10.1152/ajpendo.00405.2020
- Feng, B., Yao, P. M., Li, Y., Devlin, C. M., Zhang, D., Harding, H. P., et al. (2003). The endoplasmic reticulum is the site of cholesterol-induced cytotoxicity in macrophages. *Nat. Cell Biol.* 5, 781–792. doi:10.1038/ncb1035
- Fujii, M., Inoguchi, T., Sasaki, S., Maeda, Y., Zheng, J., Kobayashi, K., et al. (2010). Bilirubin and biliverdin protect rodents against diabetic nephropathy by downregulating NAD(P)H oxidase. *Kidney Int.* 78, 905–919. doi:10.1038/ki.2010.265
- Gazzin, S., Vitek, L., Watchko, J., Shapiro, S. M., and Tiribelli, C. (2016). A novel perspective on the biology of bilirubin in health and disease. *Trends Mol. Med.* 22, 758–768. doi:10.1016/j.molmed.2016.07.004
- Giraudi, P. J., Bellarosa, C., Coda-Zabetta, C. D., Peruzzo, P., and Tiribelli, C. (2011). Functional induction of the cystine-glutamate exchanger system Xc(-) activity in SH-SY5Y cells by unconjugated bilirubin. *PLoS One* 6, e29078. doi:10.1371/journal.pone.0029078
- Gundamaraju, R., Vemuri, R., Chong, W. C., Bulmer, A. C., and Eri, R. (2019). Bilirubin attenuates ER stress-mediated inflammation, escalates apoptosis and reduces proliferation in the LS174T colonic epithelial cell line. *Int. J. Med. Sci.* 16, 135–144. doi:10.7150/ijms.29134
- Haase, V. H. (2012). Hypoxia-inducible factor signaling in the development of kidney fibrosis. *Fibrogenesis Tissue Rep.* 5, S16. doi:10.1186/1755-1536-5-S1-S16
- Higgins, D. F., Kimura, K., Bernhardt, W. M., Shrimanker, N., Akai, Y., Hohenstein, B., et al. (2007). Hypoxia promotes fibrogenesis *in vivo* via HIF-1 stimulation of epithelial-to-mesenchymal transition. *J. Clin. Invest.* 117, 3810–3820. doi:10.1172/JCI30487
- Hinds, T. D., and Stec, D. E. (2019). Bilirubin safeguards cardiorenal and metabolic diseases: a protective role in health. *Curr. Hypertens. Rep.* 21, 87. doi:10.1007/s11906-019-0994-z
- Hinds Terry, D., and Stec David, E. (2018). Bilirubin, a cardiometabolic signaling molecule. *Hypertension* 72, 788–795. doi:10.1161/HYPERTENSIONAHA.118.11130
- Inoguchi, T., Sonoda, N., and Maeda, Y. (2016). Bilirubin as an important physiological modulator of oxidative stress and chronic inflammation in metabolic syndrome and diabetes: a new aspect on old molecule. *Diabetol. Int.* 7, 338–341. doi:10.1007/s13340-016-0288-5
- Jacobsen, J., and Wennberg, R. P. (1974). Determination of unbound bilirubin in the serum of newborns. *Clin. Chem.* 20, 783.
- Jagtap, P., and Szabó, C. (2005). Poly(ADP-ribose) polymerase and the therapeutic effects of its inhibitors. *Nat. Rev. Drug Discov.* 4, 421–440. doi:10.1038/nrd1718
- Jangi, S., Otterbein, L., and Robson, S. (2013). The molecular basis for the immunomodulatory activities of unconjugated bilirubin. *Int. J. Biochem. Cell Biol.* 45, 2843–2851. doi:10.1016/j.biocel.2013.09.014
- Kang, S. J., Lee, C., and Kruzliak, P. (2014). Effects of serum bilirubin on atherosclerotic processes. *Ann. Med.* 46, 138–147. doi:10.3109/07853890.2014.895588
- Kim, S. G., Ahn, S.-Y., Lee, E. S., Kim, S., Na, K. Y., Chae, D.-W., et al. (2014). Bilirubin activates transcription of HIF-1 α in human proximal tubular cells cultured in the physiologic oxygen content. *J. Korean Med. Sci.* 29 (Suppl. 2), S146–S154. doi:10.3346/jkms.2014.29.S2.S146
- Kimura, K., Iwano, M., Higgins, D. F., Yamaguchi, Y., Nakatani, K., Harada, K., et al. (2008). Stable expression of HIF-1 α in tubular epithelial cells promotes interstitial fibrosis. *Am. J. Physiol. Ren. Physiol.* 295, F1023–F1029. doi:10.1152/ajrenal.90209.2008
- Kume, S., and Koya, D. (2015). Autophagy: a novel therapeutic target for diabetic nephropathy. *Diabetes Metab. J.* 39, 451–460. doi:10.4093/dmj.2015.39.6.451
- Lambertucci, R. H., Hirabara, S. M., Silveira, L. D. R., Levada-Pires, A. C., Curi, R., and Pithon-Curi, T. C. (2008). Palmitate increases superoxide production through mitochondrial electron transport chain and NADPH oxidase activity in skeletal muscle cells. *J. Cell. Physiol.* 216, 796–804. doi:10.1002/jcp.21463
- Li, Y., Huang, B., Ye, T., Wang, Y., Xia, D., and Qian, J. (2020). Physiological concentrations of bilirubin control inflammatory response by inhibiting NF- κ B and inflammasome activation. *Int. Immunopharmacol.* 84, 106520. doi:10.1016/j.intimp.2020.106520
- Liu, Y., Li, P., Lu, J., Xiong, W., Oger, J., Tetzlaff, W., et al. (2008). Bilirubin possesses powerful immunomodulatory activity and suppresses experimental autoimmune encephalomyelitis. *J. Immunol. Baltim.* 181, 1887–1897. doi:10.4049/jimmunol.181.3.1887
- Maewaza, Y., Takemoto, M., and Yokote, K. (2015). Cell biology of diabetic nephropathy: roles of endothelial cells, tubulointerstitial cells and podocytes. *J. Diabetes Investig.* 6, 3–15. doi:10.1111/jdi.12255
- Mazzone, G. L., Rigato, I., Ostrow, J. D., and Tiribelli, C. (2009). Bilirubin effect on endothelial adhesion molecules expression is mediated by the NF-kappaB signaling pathway. *Biosci. Trends* 3, 151–157.
- McDonagh, A. F., and Assisi, F. (1972). The ready isomerization of bilirubin IX- in aqueous solution. *Biochem. J.* 129, 797–800.
- Mosmann, T. (1983). Rapid colorimetric assay for cellular growth and survival: application to proliferation and cytotoxicity assays. *J. Immunol. Methods* 65, 55–63.
- Nelson, T., Jacobsen, J., and Wennberg, R. P. (1974). Effect of pH on the interaction of bilirubin with albumin and tissue culture cells. *Pediatr. Res.* 8, 963–967. doi:10.1203/00006450-197412000-00010
- Oh, S. W., Lee, E. S., Kim, S., Na, K. Y., Chae, D. W., Kim, S., et al. (2013). Bilirubin attenuates the renal tubular injury by inhibition of oxidative stress and apoptosis. *BMC Nephrol.* 14, 105. doi:10.1186/1471-2369-14-105
- Ollinger, R., Bilban, M., Erat, A., Froio, A., McDaid, J., Tyagi, S., et al. (2005). Bilirubin: a natural inhibitor of vascular smooth muscle cell proliferation. *Circulation* 112, 1030–1039. doi:10.1161/CIRCULATIONAHA.104.528802
- Patten, D. A., Lafleur, V. N., Robitaille, G. A., Chan, D. A., Giaccia, A. J., and Richard, D. E. (2010). Hypoxia-inducible factor-1 activation in nonhypoxic conditions: the essential role of mitochondrial-derived reactive oxygen species. *Mol. Biol. Cell* 21, 3247–3257. doi:10.1091/mbc.E10-01-0025

- Pflueger, A., Croatt, A. J., Peterson, T. E., Smith, L. A., d'Uscio, L. V., Katusic, Z. S., et al. (2005). The hyperbilirubinemic Gunn rat is resistant to the pressor effects of angiotensin II. *Am. J. Physiol. Ren. Physiol.* 288, F552–F558. doi:10.1152/ajprenal.00278.2004
- Roca, L., Calligaris, S., Wennberg, R. P., Ahlfors, C. E., Malik, S. G., Ostrow, J. D., et al. (2006). Factors affecting the binding of bilirubin to serum albumins: validation and application of the peroxidase method. *Pediatr. Res.* 60, 724–728. doi:10.1203/01.pdr.0000245992.89965.94
- Rush, B. M., Small, S. A., Stolz, D. B., and Tan, R. J. (2018). An efficient sieving method to isolate intact glomeruli from adult rat Kidney. *J. Vis. Exp. JoVE.* doi:10.3791/58162
- Schietke, R., Warnecke, C., Wacker, I., Schödel, J., Mole, D. R., Campean, V., et al. (2010). The Lysyl oxidases LOX and LOXL2 are necessary and sufficient to repress E-cadherin in hypoxia. *J. Biol. Chem.* 285, 6658–6669. doi:10.1074/jbc.M109.042424
- Slyne, J., Slattery, C., McMorrow, T., and Ryan, M. P. (2015). New developments concerning the proximal tubule in diabetic nephropathy: *in vitro* models and mechanisms. *Nephrol. Dial. Transpl. Off. Publ. Eur. Dial. Transpl. Assoc. Eur. Ren. Assoc.* 30 (Suppl. 4), iv60–iv67. doi:10.1093/ndt/gfv264
- Stec, D. E., Storm, M. V., Pruett, B. E., and Goussset, M. U. (2013). Antihypertensive actions of moderate hyperbilirubinemia: role of superoxide inhibition. *Am. J. Hypertens.* 26, 918–923. doi:10.1093/ajh/hpt038
- Valaskova, P., Dvorak, A., Lenicek, M., Zizalova, K., Kutinova-Canova, N., Zelenka, J., et al. (2019). Hyperbilirubinemia in Gunn rats is associated with decreased inflammatory response in LPS-mediated systemic inflammation. *Int. J. Mol. Sci.* 20, 306. doi:10.3390/ijms20092306
- Vianello, E., Zampieri, S., Marcuzzo, T., Tordini, F., Bottin, C., Dardis, A., et al. (2018). Histone acetylation as a new mechanism for bilirubin-induced encephalopathy in the Gunn rat. *Sci. Rep.* 8, 13690. doi:10.1038/s41598-018-32106-w
- Vitek, L., Bellarosa, C., and Tiribelli, C. (2018). Induction of mild hyperbilirubinemia: hype or real therapeutic opportunity?. *Clin. Pharmacol. Ther.* 13, 41. doi:10.1002/cpt.1341
- Vitek, L. (2020). Bilirubin as a signaling molecule. *Med. Res. Rev.* 21, 660. doi:10.1002/med.21660
- Vitek, L., Jirsa, M., Brodanová, M., Kalab, M., Marecek, Z., Danzig, V., et al. (2002). Gilbert syndrome and ischemic heart disease: a protective effect of elevated bilirubin levels. *Atherosclerosis* 160, 449–456. doi:10.1016/s0021-9150(01)00601-3
- Vitek, L., and Ostrow, J. D. (2009). Bilirubin chemistry and metabolism; harmful and protective aspects. *Curr. Pharm. Des.* 15, 2869–2883. doi:10.2174/138161209789058237
- Wagner, K.-H., Wallner, M., Mölzer, C., Gazzin, S., Bulmer, A. C., Tiribelli, C., et al. (2015). Looking to the horizon: the role of bilirubin in the development and prevention of age-related chronic diseases. *Clin. Sci. Lond. Engl.* 129, 1–25. doi:10.1042/CS20140566
- Wallner, M., Marculescu, R., Doberer, D., Wolzt, M., Wagner, O., Vitek, L., et al. (2013). Protection from age-related increase in lipid biomarkers and inflammation contributes to cardiovascular protection in Gilbert's syndrome. *Clin. Sci. Lond. Engl.* 125, 257–264. doi:10.1042/CS20120661
- Wang, W. W., Smith, D. L. H., and Zucker, S. D. (2004). Bilirubin inhibits iNOS expression and NO production in response to endotoxin in rats. *Hepatology. Baltim. Md.* 40, 424–433. doi:10.1002/hep.20334
- Wang, Z., Tang, L., Zhu, Q., Yi, F., Zhang, F., Li, P.-L., et al. (2011). Contribution of hypoxia inducible factor-1 α to the profibrotic action of angiotensin II in cultured renal medullary interstitial cells. *Kidney Int.* 79, 300–310. doi:10.1038/ki.2010.326
- Watchko, J. F., and Tiribelli, C. (2013). Bilirubin-induced neurologic damage--mechanisms and management approaches. *N. Engl. J. Med.* 369, 2021–2030. doi:10.1056/NEJMra1308124
- Wu, D., Liu, J., Pang, X., Wang, S., Zhao, J., Zhang, X., et al. (2014). Palmitic acid exerts pro-inflammatory effects on vascular smooth muscle cells by inducing the expression of C-reactive protein, inducible nitric oxide synthase and tumor necrosis factor- α . *Int. J. Mol. Med.* 34, 1706–1712. doi:10.3892/ijmm.2014.1942
- Zelenka, J., Dvořák, A., Alán, L., Zadinová, M., Haluzík, M., and Vitek, L. (2016). Hyperbilirubinemia protects against aging-associated inflammation and metabolic deterioration. *Oxid. Med. Cell. Longev.* 60, 6190609. doi:10.1155/2016/6190609
- Zelenka, J., Lenicek, M., Muchová, L., Jirsa, M., Kudla, M., Balaz, P., et al. (2008). Highly sensitive method for quantitative determination of bilirubin in biological fluids and tissues. *J. Chromatogr. B Analyt. Technol. Biomed. Life Sci.* 867, 37–42. doi:10.1016/j.jchromb.2008.03.005
- Zennaro, C., Mariotti, M., Carraro, M., Pasqualetti, S., Corbelli, A., Armelloni, S., et al. (2014). Podocyte developmental defects caused by adriamycin in zebrafish embryos and larvae: a novel model of glomerular damage. *PLoS One* 9, e98131. doi:10.1371/journal.pone.0098131
- Zhang, K., and Kaufman, R. J. (2008). From endoplasmic-reticulum stress to the inflammatory response. *Nature* 454, 455–462. doi:10.1038/nature07203

Conflict of Interest: The authors declare that the research was conducted in the absence of any commercial or financial relationships that could be construed as a potential conflict of interest.

Copyright © 2021 Bianco, Pinci, Tiribelli and Bellarosa. This is an open-access article distributed under the terms of the Creative Commons Attribution License (CC BY). The use, distribution or reproduction in other forums is permitted, provided the original author(s) and the copyright owner(s) are credited and that the original publication in this journal is cited, in accordance with accepted academic practice. No use, distribution or reproduction is permitted which does not comply with these terms.